doi:10.1017/S1431927618003422
Microsc. Microanal. 24 (Suppl 1), 2018


# Crystal Phase Mapping by Scanning Precession Electron Diffraction and Machine Learning Decomposition

Håkon W. Ånes[1], Ingrid Marie Andersen[2] and Antonius T. J. van Helvoort[2]

[1.] Department of Materials Science and Engineering, Norwegian University of Science and Technology, Trondheim, Norway.
[2.] Department of Physics, Norwegian University of Science and Technology, Trondheim, Norway.

Analyzing the distribution of crystal phases is required to understand nanostructures. Conventional analysis in the transmission electron microscope (TEM) include acquiring dark-field (DF) images for each expected crystal phases. However, this becomes laborious if a series of phases are present, a nm-scale resolution is required and larger areas (> 0.5 $\mu m^2$) are to be analyzed. The latter is even worse for high-resolution (HR) TEM. An alternative approach is scanning precession electron diffraction (SPED), allowing for automatic determination of the crystal phase distribution. Here we combine SPED with machine learning to a model system of a ~400 nm-thick GaAs nanowire (NW) with multiple axial GaAsSb-based superlattices [1].

A JEOL 2100F TEM, equipped with a NanoMEGAS ASTAR system [2] for SPED acquisition and a bottom mounted 2k Gatan Ultrascan CCD for conventional analysis was used. For SPED, a 1 nm-probe precessed at 0.5$^o$ was scanned at 3.2 nm-steps across a 0.67 x 1.25 $\mu m^2$ area of the NW including a superlattice, while one PED pattern per position was collected with an exposure time of 10 ms. The NW was oriented with the phase boundaries parallel to the beam, i.e. at the <110> zone, to avoid overlapping phases in the beam direction. The four-dimensional data set was analyzed using the HyperSpy [3] Python library, with machine learning decomposition performed on a computer cluster.

The selected area electron diffraction (SAED) pattern in Fig. 1(a) reveals the presence of the zinc-blende (ZB) phase in two twin-related orientations (labelled ZB1 and ZB2) and one wurtzite (WZ) phase. The $111_{ZB1}$ DF image in (c) shows the spatial distribution of ZB1. The HRTEM image in (b) depicts a mixed stacking between the larger ZB segments. These finer details are partly resolved in the virtual DF (VDF) images in (g,j), formed by summing the intensities within the virtual aperture in (d) for the stack of patterns. This indicates a spatial resolution of ~3-4 nm for the chosen parameters. Precession reduces intensity variations due to thickness and bending, as seen when comparing (c) and (g). Diffraction patterns can also be collected from thick regions (~400 nm) as shown in (i). Template matching to simulated patterns [2] is problematic in the present case due to thickness variations and the data file size. To automatically examine the present phases, non-negative matrix factorization (NMF) was applied to the SPED stack, as this was demonstrated as a suitable approach to automatic phase identification [4].

To learn the number of required 'component patterns' to describe the data and identify the three phases, decompositions with three to 15 components were performed. For the total scanned area, the number could not be estimated directly by analyzing the proportion of variance in principal component analysis (PCA) components as shown in Fig. 2(a). This is possibly due to the NW bending over the scanned length more than the precession angle used and the large thickness variations. The resultant component patterns and their associated NMF 'loadings' were analyzed by comparison to conventional TEM results in Fig. 1. A minimum of six components was required to get one component for each expected phase. A combined RGB loading with the corresponding component patterns is given in Fig. 2(b,c). Other components were

related to vacuum, C-support film and dynamical diffraction in thicker regions (> 75 nm). No individual WZ component was identified in decompositions with fewer than six components, while for more components single phases were separated into multiple components. For decompositions with more components, the additional ones can be related to NW bending and thickness effects. The latter can be used to evaluate the kinematic approximation for SPED, as illustrated in Fig. 1(h,i).

Further work includes extending the scan area while retaining the required resolution and minimizing unnecessary scanned area (as e.g. vacuum and C-support) to reduce the number of decomposition components to the NW phases only. An alternative and objective approach to PCA for an evaluation criterion for selecting the present 'component patterns' must be found, and other statistical decompositions such as data clustering [5] should be evaluated [6].

References:
[1] D Ren *et al*, ArXiv preprint (2017), 1708.06971.
[2] P Moeck *et* al, Cryst. Res. Technol. **46** (2011), p. 589-606.
[3] F de la Peña *et al*, Hyperspy 1.3 Zenodo. https://doi.org/10.5281/zenodo.583693, (2017).
[4] A S Eggeman *et al*, Nat. Commun. **6** (2015), p. 7267.
[5] B Martineau *et al*, Microsc. Microanal. **23** (Suppl 1) (2017), p. 116-117.
[6] Acknowledgements: The Research Council of Norway's support for NORTEM (197405).

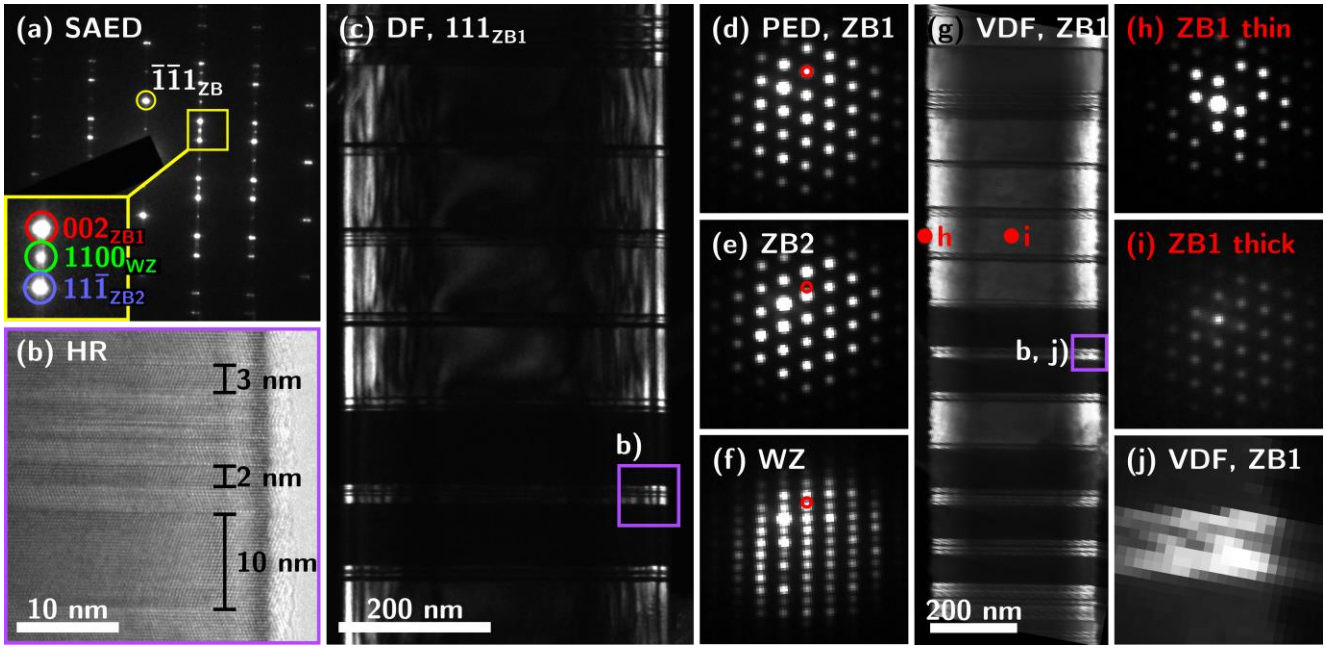


**Figure 1.** (a-c) Comparison of conventional TEM analysis and (d-j) SPED.

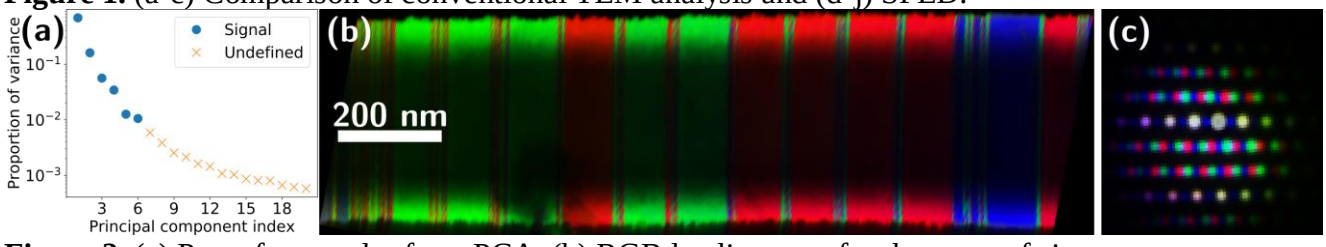


**Figure 2.** (a) Part of scree plot from PCA. (b) RGB loading map for three out of six components representing present NW phases. (c) Corresponding RGB component patterns.


https://doi.org/10.1017/S1431927618003422